Tumor Biol. (2016) 37:5857–5867
DOI 10.1007/s13277-015-4439-2

ORIGINAL ARTICLE

# Irradiation induces glioblastoma cell senescence and senescence-associated secretory phenotype

**Hee-Young Jeon[1,2] · Jun-Kyum Kim[1,2] · Seok Won Ham[1] · Se-Yeong Oh[3] · Jaebong Kim[4] · Jae-Bong Park[4] · Jae-Yong Lee[4] · Sung-Chan Kim[4] · Hyunggee Kim[1,2]**

Received: 24 August 2015 / Accepted: 12 November 2015 / Published online: 19 November 2015


**Abstract** Glioblastoma multiforme (GBM) is one of the most aggressive and fatal primary brain tumors in humans. The standard therapy for the treatment of GBM is surgical resection, followed by radiotherapy and/or chemotherapy. However, the frequency of tumor recurrence in GBM patients is very high, and the survival rate remains poor. Delineating the mechanisms of GBM recurrence is essential for therapeutic advances. Here, we demonstrate that irradiation rendered 17–20 % of GBM cells dead, but resulted in 60–80 % of GBM cells growth-arrested with increases in senescence markers, such as senescence-associated beta-galactosidase-positive cells, H3K9me3-positive cells, and p53-p21$^{CIP1}$-positive cells. Moreover, irradiation induced expression of senescence-associated secretory phenotype (SASP) mRNAs and NFκB transcriptional activity in GBM cells. Strikingly, compared to injection of non-irradiated GBM cells into immune-deficient mice, the co-injection of irradiated and non-irradiated GBM cells resulted in faster growth of tumors with the histological features of human GBM. Taken together, our findings suggest that the increases in senescent cells and SASP in GBM cells after irradiation is likely one of main reasons for tumor recurrence in post-radiotherapy GBM patients.

**Keywords** Glioblastoma multiforme · Radiotherapy · Recurrence · Senescence · Senescence-associated secretory phenotype

**Electronic supplementary material** The online version of this article (doi:10.1007/s13277-015-4439-2) contains supplementary material, which is available to authorized users.

✉ Sung-Chan Kim
biokim@hallym.ac.kr

✉ Hyunggee Kim
hg-kim@korea.ac.kr

[1] Department of Biotechnology, School of Life Sciences and Biotechnology, Korea University, Seoul, Republic of Korea

[2] Institute of Animal Molecular Biotechnology, Korea University, Seoul, Republic of Korea

[3] Institute of Life Science and Natural Resources, Korea University, Seoul, Republic of Korea

[4] Department of Biochemistry, Institute of Cell Differentiation and Aging, College of Medicine, Hallym University, Chuncheon, Republic of Korea

## Introduction

Glioblastoma multiforme (GBM) is one of the most aggressive and common primary brain tumors. Radiotherapy is part of the conventional therapy that is currently used to eradicate GBM with administration of temozolomide after surgical removal of the tumor. Unfortunately, the median survival period of patients with GBM remains less than 2 years due to its high recurrence frequency after treatment [1–3]. Because the sites of recurrence of post-radiotherapy GBM are located around the radiation-treated areas [4, 5], it is thought that radiation may lead to the induction of a tumor-promoting microenvironment. Many studies have focused on developing potent and effective radio-sensitizers or anti-tumor drugs to be used in combination with radiotherapy [6–9].

Irradiated cells activate their DNA damage checkpoints to delay cell cycle progression in an ATM/ATR-activation manner. Activated ATR/ATM phosphorylates p53 to induce G1 cell cycle arrest. The phosphorylated p53 increases the expression of p21$^{CIP1}$, an endogenous inhibitor of cyclin-dependent kinases, to trigger cell growth arrest, senescence, or apoptosis [10–12]. Senescent cells express senescence-associated beta-

galactosidase (SA-β-gal) and present a flat and enlarged morphology. Furthermore, senescent cells show irreversible cell cycle arrest with a metabolically active state. One study reported that tumor cells can undergo senescence following treatment with radiation and chemotherapeutic agents in vitro and in vivo [13]. In addition, other studies also showed the changes of gene expression and senescence-like cellular phenotype after radiation in several cancer models [14, 15]. Tumor cells may follow the senescence process as a defense mechanism against tumor progression [16–19].

Recent evidence suggests that senescent cells may express the senescence-associated secretory phenotype (SASP), which includes growth factors, cytokines, and other factors such as monocyte chemotactic protein 1 (MCP1), chemokine C-X-C motif ligand 1 (GRO1), and $p21^{CIP1}$ [12, 13, 20, 21]. Some studies reported that SASP is required for induction and maintenance of senescence phenotype in normal cells [19, 22], while the radiation-induced senescent breast cancer cells express the SASP that is required for triggering the proliferation, invasion, and migration of surrounding cells in vitro [23, 24]. It is also known that senescent cells secrete interleukin 6 (IL6) and IL8, which can stimulate the invasion of premalignant cells, leading to a secondary tumor [25]. These studies suggest that radiotherapy-induced senescence can promote the progression and invasion of tumors in vivo.

In the present study, our aim was to elucidate role of radiation in GBM cells, and we found that irradiation leads to GBM cell senescence and SASP expression in vitro, and irradiated GBM cells promote tumor progression in non-irradiated GBM cells in in vivo tumor xenografts.

## Materials and methods

### Cells and culture conditions

Human GBM cell lines U87MG (*p53*wt, *PTEN*mut, *p14ARF*/*p16*del) and LN229 (*p53*mut, *PTEN*wt, *p14ARF*/*p16*del) were purchased from the American Type Culture Collection (ATCC, Manassas, VA, USA) and cultured in high-glucose Dulbecco's Modified Eagle's medium (DMEM) supplemented with 10 % fetal bovine serum (Serana, Bunbury, Australia), 1 % penicillin/streptomycin (Lonza, Basel, Switzerland), and 2 mM L-glutamine (Lonza) at 37 °C with 5 % $CO_2$ and 95 % humidity.

### Plasmids and lentiviral infection

U87MG and LN229 cells were infected with lentivirus produced from 293FT cell line (Life Technologies) that was transfected with a lentiviral vector (pLL-CMV-puro, pLL-CMV-IκBα mutant-puro, and pCDH-CMV-EF1-DsRed) and packaging vectors (3rd generation: pMDLg/pRRE, pRSV-Rev, and pMD2.G).

### $^{137}$Cs γ-ray irradiation

$^{137}$Cs γ-ray irradiation at a dose rate of 2.04 Gy/min for a total dose of 20 Gy was conducted using an IBL 437C (CIS Bio-International, Codolet, France).

### Cell counting

To assess proliferation, cells were irradiated with 20 Gy, and then $1 \times 10^4$ cells were plated in 6-well plates. The cells were harvested by trypsin digestion and stained with trypan blue to exclude dead cells. Then, live cells were counted using a hemocytometer on days 1, 3, 5, and 7.

### Annexin V and propidium iodide staining

Non-irradiated or irradiated GBM cells were grown for 3 days. GBM cells were treated with bis-chloroethylnitrosourea (BCNU; 80 μg/mL) for 1 day. Then, cells were collected and washed twice with phosphate-buffered saline (PBS). Irradiated, non-irradiated and BCNU-treated cells were incubated with Annexin V-FITC (BD Bioscience, Bedford, MA, USA) with or without propidium iodide (PI) (BD Bioscience) for 15 min at room temperature in the dark. Incubated cells were analyzed by fluorescence-activated cell sorting (FACSVerse, BD Bioscience).

### 5-Bromo-2′-deoxyuridine incorporation assay

Non-irradiated or irradiated glioma cells were seeded in 24-well plates for 3 days and then incubated with 10 μM 5-Bromo-2′-deoxyuridine (BrdU) (B5002, Sigma-Aldrich, St. Louis, MO, USA)-containing media for 3 h. Next, cells were harvested by trypsin digestion, and collected cells were washed twice with PBS and fixed in 4 % paraformaldehyde (PFA) for 15 min at room temperature. Then, cells were washed twice with cold PBS and incubated with 2 M HCl for 45 min followed by 0.1 M borate buffer for 15 min at room temperature. Next, cells were treated with anti-BrdU (1:500; 347583, BD Bioscience) antibody for 12 h at 4 °C. Fluorescence images were obtained using an upright fluorescence microscope (Axio Imager M1, Carl Zeiss, Oberkochen, Germany).

### Carboxyfluorescein succinimidyl ester dilution assay

For labeling with carboxyfluorescein succinimidyl ester (CFSE) (Sigma-Aldrich), GBM cells were harvested and centrifuged to pellet the cells. Then, cells were washed with PBS and incubated with CFSE solution for 30 min at room temperature. Next, cells

were centrifuged, the supernatants aspirated, and the cells suspended in culture media. Harvested cells were analyzed on days 1, 4, and 7 using the FACSCalibur (BD Bioscience).

### SA-β-gal staining

To detect cell senescence, non-irradiated or irradiated GBM cells were stained using a Senescence β-Galactosidase Staining Kit (9860, Cell Signaling Technology, Danvers, MA, USA), according to the manufacturer's instructions. In brief, after washing the plate with PBS, 1× fixative solution was added to each well, and the plate was incubated for 15 min at room temperature. Next, the plate was rinsed with PBS followed by adding β-galactosidase staining solution. Then, the plate was incubated overnight at 37 °C in a dry incubator (no $CO_2$). After incubation, cells were analyzed using an inverted fluorescence microscope (Axio Observer D1, Carl Zeiss) to detect the blue color.

### Immunofluorescence assay

Non-irradiated or irradiated glioma cells were seeded in 24-well plates for 3 days. Then, cells were fixed in 4 % PFA and incubated with primary anti-p21 (1:200; sc-397, Santa Cruz Biotechnology, Dallas, TX, USA), anti-H3K9me3 (1:200; 07–442, EMD Millipore, Bedford, MA, USA) antibodies for 12 h at 4 °C. Cells were washed twice with PBS and incubated with fluorescence-conjugated secondary antibody (Invitrogen, Carlsbad, CA, USA) for 1 h at room temperature. Cells were then counterstained with the nuclear dye 4′,6-diamidino-2-phenylindole (DAPI; 1 μg/mL) for 5 min. Fluorescence images were obtained using the Axio Imager M1 microscope.

### Quantitative reverse transcription-polymerase chain reaction

Quantitative reverse transcription-polymerase chain reaction (qRT-PCR) was performed in order to determine the mRNA levels. Total RNA was isolated from cells using TRIzol Reagent (Invitrogen), according to the manufacturer's instructions. RNA (1 μg) that had been treated with RNase-free DNase was utilized as a template for synthesizing complementary DNA (cDNA) using the RevertAid First Strand cDNA Synthesis Kit (Thermo Scientific, Waltham, MA, USA), according to the manufacturer's instructions. The qRT-PCR analysis was performed using Takara Bio SYBR Premix Ex Taq and CFX096 (Bio-Rad, Hercules, CA, USA). The expression level of each target gene was normalized to that of 18S rRNA. The primer sequences were human 18S rRNA forward: 5′-CAGCCACCCGAGATTGAGCA-3′, reverse: 5′-TAGTAGCGACGGGCGGTGTG-3′, human MCP1 forward: 5′-CCCAAACTCCGAAGACTTGA-3′, reverse: 5′-CAAAACATCCCAGGGGTAGA-3′, human GRO1 forward: 5′-AATCCAACTGACCAGAAGGG-3′, reverse: 5′-CATTAGGCACAATCCAGGTG-3′, human IL6 forward: 5′-CCTGAACCTTCCAAAGATGGC-3′, reverse: 5′-TTCACCAGGCAAGTCTCCTCA-3′, human IL8 forward: 5′-GCTCTGTGTGAAGGTGCAGT-3′, reverse: 5′-ACTTCTCCACAACCCTCTGC-3′, human VEGFA forward: 5′-AGGGCAGAATCATCACGAAGT-3′, reverse: 5′-AGGGTCTCGATTGGATGGCA-3′, human CSF1 forward: 5′-GCT CCAGGAGTCTGTCTTCC-3′, reverse: 5′-GTAGAACAAGAGGCCTCCGA-3′, human CXCL12 forward: 5′-ATTCTCAACACTCCAAACTGT-3′, reverse: 5′-CACTTTAGCTTCGGGTCAATGC-3′, human p21 forward: 5′-TTAGCAGCGGAACAAGGAGT-3′, reverse: 5′-ATTCAGCATTGTGGGAGGAG-3′, human EGF forward: 5′-CTCCATGATGGTGTGTGCAT-3′, reverse: 5′-ACCCCCATTCTTGAGGTCTT-3′, human FGF2 forward: 5′-ACCGGTCAAGGAAATACACC-3′, reverse: 5′-CAGCTCTTAGCAGACATTGGA-3′, human IL1α forward: 5′-CAGCCAGAGAGGGAGTCATT-3′, reverse: 5′-GGAGTGGGCCATAGCTTACA-3′, human IL1β forward: 5′-CCCAACTGGTACATCAGCAC-3′, and reverse: 5′-GGAAGACACAAATTGCATGG-3′.

### Western blot analysis

Cell extracts were prepared using RIPA lysis buffer (150 mM sodium chloride, 1 % NP-40, 0.1 % SDS, 50 mM Tris, pH 7.4) containing 1 mM β-glycerophosphate, 2.5 mM sodium pyrophosphate, 1 mM sodium fluoride, 1 mM sodium orthovanadate, and protease inhibitor (Roche, Basel, Switzerland). Protein concentration was quantified using the Bradford assay reagent (Bio-Rad), according to the manufacturer's instructions. Proteins were resolved by SDS-PAGE and then transferred to a polyvinylidene fluoride membrane (Pall Corporation, Port Washington, NY, USA). Membranes were blocked with 5 % nonfat milk and incubated with the following antibodies at the indicated dilutions: anti-p21 (1:500; sc-397), anti-IκBα (1:500; sc-371), anti-p53 (1:500; sc-126, all from Santa Cruz Biotechnology), anti-p-p53 (1:500; 9286, Cell Signaling Technology), and anti-β-actin (1:10,000; A5316, Sigma-Aldrich). Membranes were then incubated with horseradish peroxidase-conjugated anti-IgG secondary antibody (Pierce Biotechnology, Rockford, IL, USA) and visualized using the SuperSignal West Pico Chemiluminescent Substrate (Pierce Biotechnology).

### Luciferase assay

NFκB-regulated promoter/luciferase gene activity was determined in GBM cells by transfection of NFκB (which contains multiple NFκB binding sites in the promoter of the firefly luciferase reporter gene) plasmid using the Dual-Glo Luciferase Assay System (Promega, Madison, WI, USA).

Transfection efficiency was normalized to the activity of Renilla luciferase according to the manufacturer's instructions.

### Subcutaneous glioma cell implantation and tumor dissociation

GBM cells were injected subcutaneously into nude mice (BALB/c nu/nu). Mice were sacrificed when the tumor size exceeded 1500 $mm^3$, and the tumors were harvested. All mouse experiments were approved by the Animal Care Committee of the College of Life Sciences and Biotechnology, Korea University, according to government and institutional guidelines and regulations of Korea. The tumors were minced into 2–4 mm fragments and then incubated with trypsin for 30 min at 37 °C. The fragments were filtered through a 40 μm nylon mesh cell strainer (CD1-1KT, Sigma-Aldrich). The released cells were centrifuged at 1200 rpm for 3 min and incubated in culture media at 37 °C with 5 % $CO_2$ and 95 % humidity [26].

### Hematoxylin and eosin and Ki67 staining in tumor tissue

Tumor-bearing mice were perfused with PBS and 4 % PFA. Obtained tumor tissues were embedded in paraffin, sectioned (4 μm in thickness), and placed on glass slides. After deparaffinization and hydration, the tissue slides were treated with hematoxylin (Merck, Darmstadt, Germany) for 5 min and rinsed with tap water. Next, tissue slides were dipped 10–15 times in acidic alcohol and rinsed again in tap water. All slides were incubated in an eosin solution (109844, Merck) for 30 s, followed by washing with distilled water.

After deparaffinization and hydration, the tissue slides were stained with primary antibodies against Ki67 (NCL-Ki67p, Leica Biosystems, UK) for 12 h at 4 °C. Cells were washed twice with PBS and incubated with fluorescence-conjugated secondary antibody (Invitrogen) for 1 h at room temperature. Nuclei were then stained with DAPI (1 μg/mL) for 5 min. Fluorescence images were obtained using a confocal laser scanning microscope (LSM5 Pascal, Carl Zeiss).

### Statistical analysis

Statistical analysis was performed using the two-tailed Student's *t* test. Values of $p < 0.05$ (*) or $p < 0.01$ (**) were considered statistically significant for different experiments, as indicated in the figure legends. Data are presented as means ±standard error of the mean (SEM).

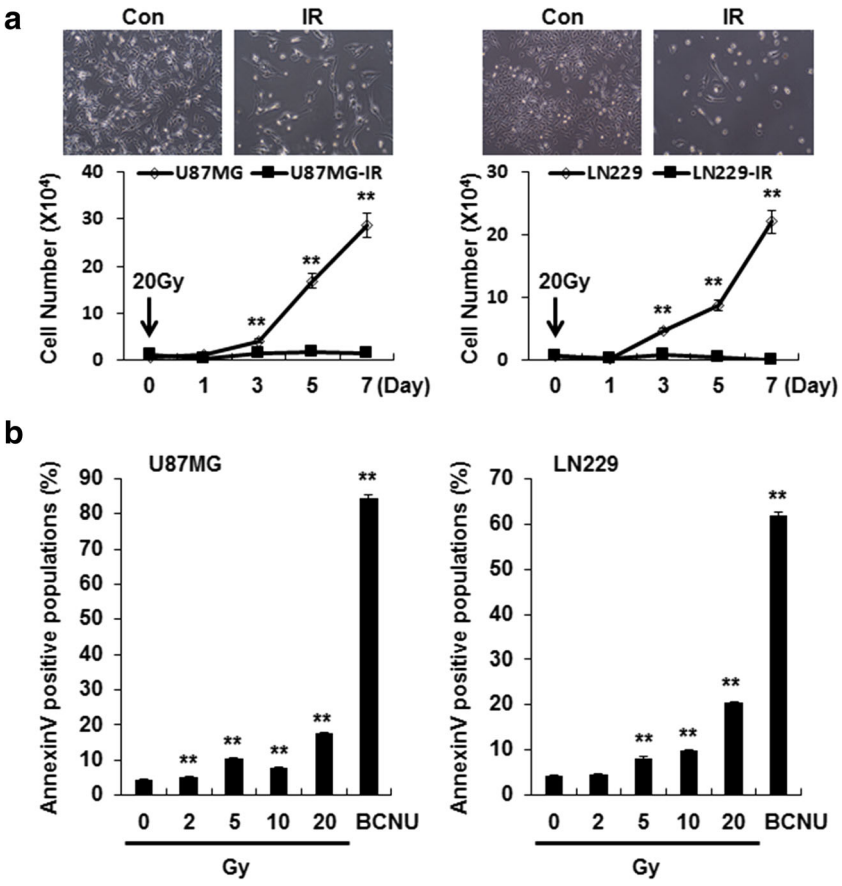


**Fig. 1** Irradiation promotes GBM cell growth inhibition rather than cell death. **a** Upper panel shows representative images of irradiated U87MG and LN229 and non-irradiated control cells on day 7 after irradiation with 20 Gy. Lower panels show GBM cell proliferation after irradiation with 20 Gy. Irradiation led to growth inhibition in U87MG and LN229 cells in a time-dependent manner compared to non-irradiated control cells. $^{**}p<0.01$ ($n=3$). Data are expressed as means± SEM. **b** FACS analysis revealed that Annexin V-positive U87MG and LN229 apoptotic cells gradually increased in a radiation dose-dependent manner on day 3. However, total apoptotic cells after irradiation were less than 17 and 20 % in U87MG and LN229 cells, respectively. BCNU-treated U87MG and LN229 cells were used for positive controls of cellular apoptosis. $^{*}p<0.05$, $^{**}p<0.01$ ($n=3$). Data are expressed as means±SEM

## Results

### Irradiation influences GBM cell growth rather than cell death

To determine whether irradiation induces death in GBM cells, we exposed the GBM cell lines U87MG and LN229 to 20 Gy of radiation and found that irradiation significantly inhibited the growth of U87MG and LN229 cells during 7 days after exposure (Fig. 1a). Next, we tested whether irradiation triggers cellular apoptosis by exposing cells to various doses of radiation (0 to 20 Gy). We used BCNU-treated U87MG and LN229 cells as positive controls for cellular apoptosis (Fig. 1b; 84.6 and 61.9 % cell death in BCNU-treated U87MG and LN229 cells, respectively). Annexin V-FITC analysis showed that irradiation did not markedly induce apoptosis after exposure of up to 20 Gy (Fig. 1b; 17 and 20 % cell death in irradiated U87MG and LN229 cells, respectively). Therefore, our results indicate that irradiation results in inhibition of GBM cell growth rather than induction of cell death.

### Irradiation leads to GBM cell cycle arrest

To further determine the effect of irradiation on the proliferative ability of U87MG and LN229 cells, we performed a BrdU incorporation assay and CFSE dilution assay. The BrdU incorporation assay revealed that irradiation markedly inhibited the proliferation of GBM cells and significantly decreased the number of BrdU-positive cells at different time periods after exposure to 20 Gy (Fig. 2a). The CFSE dilution assay also showed that the CFSE dye was rapidly diluted depending on the proliferation of non-irradiated GBM cells, but was diluted slowly in irradiated GBM cells (Fig. 2b). These results suggest that irradiated GBM cells undergo cell cycle arrest in the G0 or G1 phase.

### Irradiation induces GBM cell senescence

Based on our results from the CFSE dilution assay, we assumed that irradiation may induce cellular senescence in GBM cells. To test our hypothesis, we first observed the GBM cell morphology and found that irradiation caused

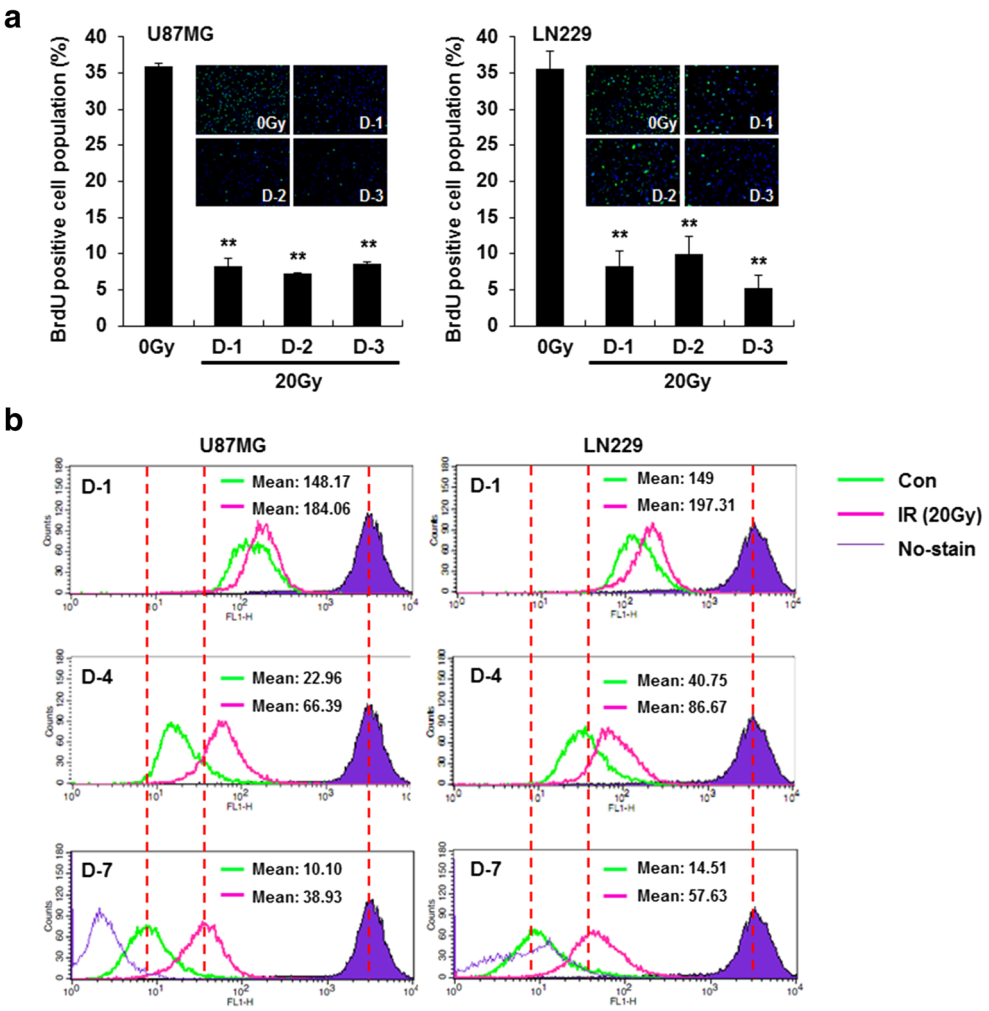


**Fig. 2** Irradiated GBM cells undergo growth arrest. **a** The BrdU incorporation assay revealed that the proliferation of U87MG and LN229 cells is significantly inhibited by irradiation with 20 Gy compared to non-irradiated counterpart cells. $^{**}p<0.01$ ($n=3$). Data are expressed as means±SEM. **b** U87MG and LN229 cells were cultured with the fluorescent dye CFSE and harvested at indicated time points (days 1, 4, and 7) after irradiation with 20 Gy or without irradiation. FACS analysis showed that CFSE was rapidly diluted out depending on the proliferation of non-irradiated GBM cells, but diluted slowly in irradiated GBM cells

significant changes, including cell enlargement, a larger flattened cytoplasm, and vacuole formation, compared to non-irradiated GBM cells (Fig. 3a). These changes represent the induction of senescence in GBM cells. Furthermore, we detected SA-β-gal activity, a surrogate marker of senescence. Interestingly, SA-β-gal-positive cell populations were significantly increased in U87MG and LN229 cells in a radiation dose-dependent manner (Fig. 3b, c). Taken together, these results indicate that irradiation induces senescence in GBM cells.

### Irradiation induces senescence markers in GBM cells

Next, we performed a number of biochemical analyses to further confirm irradiation-induced senescence in GBM cells. A relatively high population of H3K9me3-positive cells, a marker of senescent cells with heterochromatin DNA, was observed in the irradiated GBM cells compared to the non-irradiated counterpart cells (Fig. 4a). Cells expressing $p21^{CIP1}$, a well-known senescence marker, were relatively high among irradiated GBM cells (Fig. 4b). Moreover, the $p21^{CIP1}$ mRNA levels in U87MG and LN229 cells were also increased in a time-dependent manner after irradiation (Fig. 4c, d). It is known that the U87MG cell line has the wild-type *p53* gene and LN229 cells contain a mutant *p53* gene with normal p53 function [27]. The p53 transcription factor is phosphorylated by irradiation-induced DNA damage and activates cell cycle checkpoints by increasing $p21^{CIP1}$ expression [28]. Therefore, we performed a Western blot assay to measure total and phosphorylated p53 protein levels. The results show that total and phosphorylated p53 and $p21^{CIP1}$ markedly increased in irradiated GBM cells compared to non-irradiated counterpart cells (Fig. 4e, f). Taken together, these results suggest that the p53-$p21^{CIP1}$ regulatory axis is likely associated with cellular senescence rather than apoptosis in the irradiated GBM cells.

### Irradiation increases SASP and NFκB transcriptional activity in GBM cells

Senescent cells are metabolically active and able to crosstalk with other cells through several secretory factors, which is also known as SASP. We examined the mRNA levels of SASP in irradiated GBM cells by using qRT-PCR. The results show that the SASP factors MCP1, GRO1, IL6, IL8, IL1α, IL1β, and $p21^{CIP1}$ significantly increased in irradiated U87MG and LN229 cells compared to non-irradiated counterpart cells

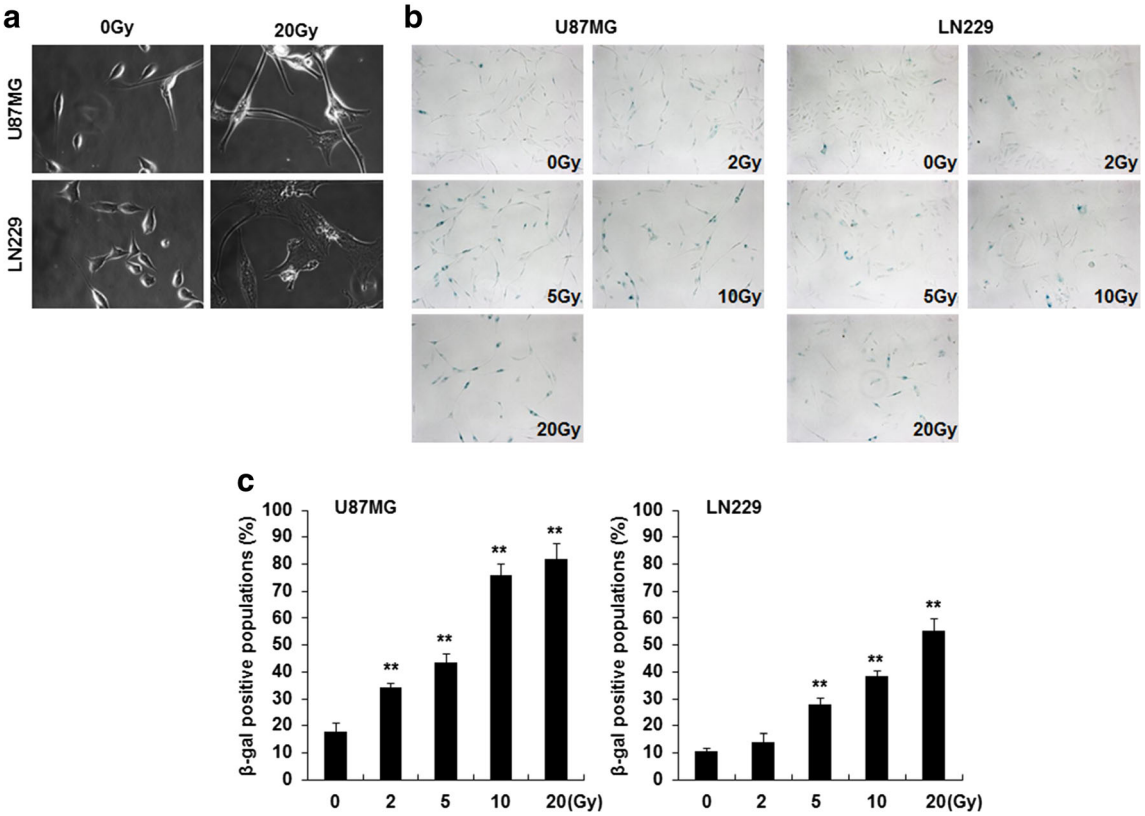


**Fig. 3** Irradiation induces GBM cell senescence. **a** U87MG and LN229 cells displayed morphological changes, such as cell flattening and enlargement, after irradiation. The images shown were obtained on day 3 after irradiation with 20 Gy. **b** The SA-β-gal staining assay revealed that irradiation renders the majority of U87MG and LN229 cells SA-β-gal-positive. The representative photos shown were obtained from GBM cells treated with indicated radiation doses on day 3. **c** The graphs indicate quantitative data for SA-β-gal-positive GBM cells shown in Fig. 3b. $^{**}p<0.01$ ($n=3$). Data are expressed as means±SEM

(Fig. 5a). NFκB signaling is known to be a master regulator for SASP induction [29]. Therefore, we analyzed the expression level of IκBα, an endogenous inhibitor of the transcription factor NFκB. The results show that IκBα protein levels markedly decreased in GBM cells in a time-dependent manner after irradiation (Fig. 5b), indicative of NFκB activation. To directly evaluate NFκB signaling, we analyzed the promoter/luciferase reporter gene activity of the transcription factor NFκB. The results show that irradiation enhanced the NFκB promoter transcriptional activity in U87MG and LN229 cells (Fig. 5c). Collectively, these results suggest that irradiation likely triggers SASP induction in GBM cells through the activation of NFκB signaling.

To understand a direct role of NFκB in the irradiation-induced senescence and cell death, we established U87MG and LN229 cell lines expressing IκBα mutant that constitutively inhibit NFκB by escaping from IκB kinase-mediated phosphorylation and subsequent degradation. We found that there was no significant difference in SA-β-gal activity between the control and IκBα mutant-expressing GBM cells (data not shown). However, apoptotic cell population was relatively decreased in IκBα mutant-expressing GBM cells compared to control cells by irradiation (sFig. 1). Therefore, these results indicate that NFκB signaling is not directly linked to radiation-induced cell autonomous senescence.

## In vivo tumor xenograft growth of GBM cells is elevated when co-injected with irradiated GBM cells

Because most SASP genes induced in irradiated GBM cells are associated with tumor initiation and progression, we speculated that irradiated cells are implicated in tumor recurrence after radiotherapy. To test our assumption, we established an in vivo xenograft experimental model by which the role of

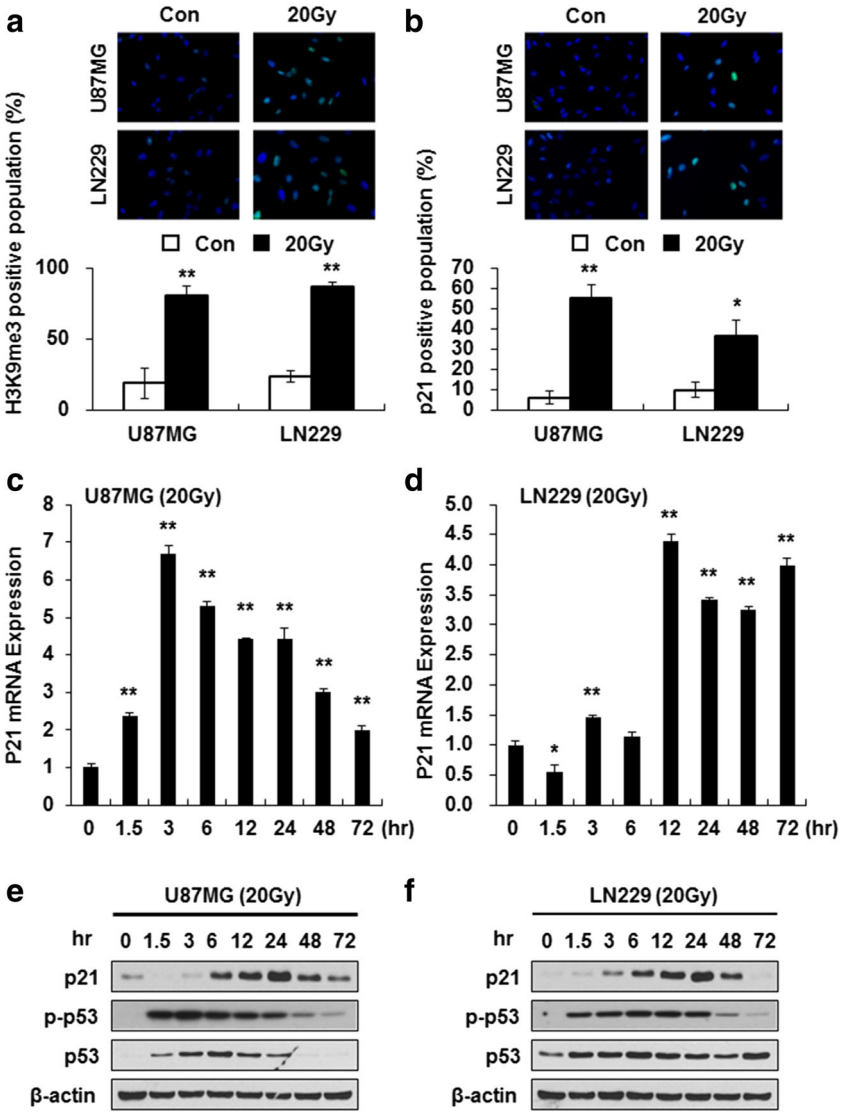


**Fig. 4** Irradiation increases the expression of senescence markers in GBM cells. **a** Immunofluorescence analysis revealed that H3K9me3, the heterochromatin DNA and senescence marker, was significantly increased in the U87MG and LN229 cells on day 3 after irradiation with 20 Gy. $^{**}p<0.01$ ($n=3$). Data are expressed as means±SEM. **b** Immunofluorescence analysis showed that $p21^{CIP1}$, an important senescence inducer, was markedly increased in nuclei of U87MG and LN229 cells on day 3 after irradiation with 20 Gy. $^{*}p<0.05$, $^{**}p<0.01$ ($n=3$). Data are expressed as means±SEM. **c** and **d** qRT-PCR assay showed that $p21^{CIP1}$ mRNA was increased in U87MG and LN229 cells at the indicated time points after irradiation with 20 Gy. $^{*}p<0.05$, $^{**}p<0.01$ ($n=3$). Data are expressed as means±SEM. **e** and **f** Western blot analysis revealed that $p21^{CIP1}$, total p53, and phosphorylated p53 protein levels increased in U87MG and LN229 cells at the indicated time points after irradiation with 20 Gy

irradiated GBM cells in tumor progression is evaluated by co-injection with non-irradiated GBM cells and irradiated GBM cells that express the red fluorescent protein DsRed. The results show that $2\times10^6$-irradiated U87MG-DsRed and LN229-DsRed cells alone did not form a tumor mass in immune-deficient mice (Fig. 6a, d). Of interest, co-injection of $1\times10^6$ U87MG cells with $2\times10^6$-irradiated U87MG-DsRed cells produced relatively large tumors compared to $1\times10^6$ U87MG cells alone (Fig. 6a, b). Similarly, co-injection of $1\times10^6$ LN229 cells with $2\times10^6$-irradiated LN229-DsRed cells generated larger tumor volume and mass than $1\times10^6$ LN229 cells alone (Fig. 6d, e). We then harvested the subcutaneous tumor masses and stained them with hematoxylin and eosin (H&E) and Ki67 to evaluate their histological features. The H&E revealed that tumors derived from co-injected irradiated and non-irradiated cells displayed relatively more aggressive GBM phenotypes, including cells with diverse sizes, increased vessel formation, and palisading necrosis, compared to tumors obtained from injected non-irradiated cells (Fig. 6c, f). However, Ki67 staining analysis revealed that there was no obvious difference in cell proliferation in tumors derived from two the groups (Fig. 6c, f). To examine whether irradiated DsRed-positive senescent cells are present in the tumors, we dissociated the tumor into single cells and analyzed the existence of DsRed-positive cell populations by FACS analysis. Compared to DsRed fluorescence-positive cell population from $1\times10^6$ non-irradiated LN229 cells with $2\times10^6$-irradiated LN229-DsRed cells before the mouse co-injection (sFig. 2a), there were no irradiated DsRed-positive LN229 cells in the single cells derived from the tumors (sFig. 2b). These results indicate that the irradiated GBM cells should be disappeared after changing tumor microenvironment.

Taken together, our findings suggest that irradiation may influence GBM progression and recurrence by generating a tumor-promoting microenvironment that stimulates growth of irradiation-escaped GBM cells after radiotherapy treatment.

## Discussion

Although many cancer biologists have focused on delineating the molecular mechanism underlying tumor recurrence, the exact mechanism has remained elusive. Several studies have reported that senescence is a physiological defense mechanism that suppresses tumor progression at a premalignant stage [30, 31]. However, it has also been reported that senescence can promote the initiation and progression of cancer [12, 13]. For example, soluble factors secreted by senescent cells can promote the growth of premalignant and malignant epithelial cells [32]. In addition, tumor tissues develop cellular senescence after administration of radiation therapy and chemotherapeutic agents in vitro and in vivo [13]. Several other

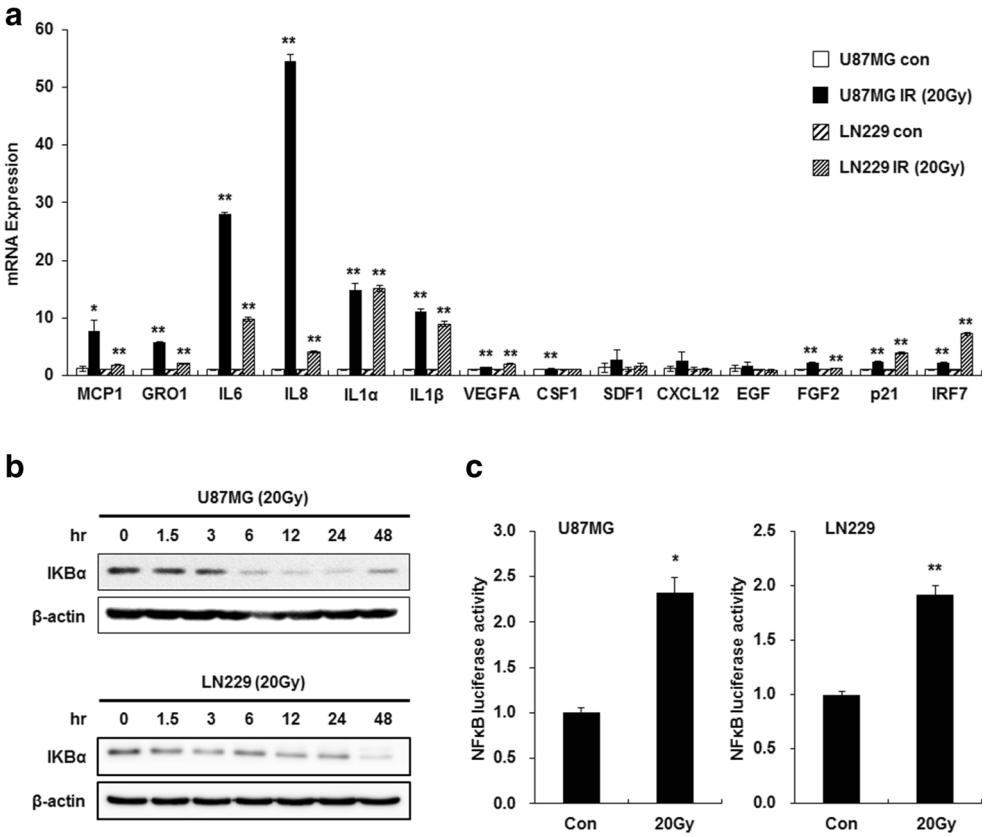


**Fig. 5** Irradiation induces expression of SASP and NFκB activity in GBM cells. **a** qRT-PCR assay showed that mRNA levels of the SASP genes MCP1, GRO1, IL6, IL8, IL1α, and IL1β were significantly increased in the U87MG and LN229 cells on day 3 after irradiation with 20 Gy. *$p<0.05$, **$p<0.01$ ($n=3$). Data are expressed as means±SEM. **b** Western blot analysis revealed that IκBα protein levels gradually decreased in U87MG and LN229 cells in a time-dependent manner after irradiation with 20 Gy. **c** The promoter/luciferase reporter gene assay showed that NFκB promoter transcriptional activity was significantly increased in the U87MG and LN229 cells 24 h after irradiation with 20 Gy. *$p<0.05$, **$p<0.01$ ($n=3$). Data are expressed as means±SEM

studies have also suggested that cellular senescence is a promising target to eradicate cancer and reduce the incidence of tumor recurrence [16, 19, 29]. Therefore, it is likely that, in the early stages of tumor development, cellular senescence may be acquired as a defense mechanism against tumor cells, while in late stages of tumor development or in a tumor after therapy, cellular senescence may lead to tumor progression.

The traditional therapy against GBM now in use is the concomitant treatment by radiotherapy with chemotherapeutic agents after surgical resection [33]. Recently, Kioi et al. [34] reported that bone marrow-derived cells (BMDCs) are recruited to GBM and promote neovasculogenesis after radiotherapy treatment. Furthermore, the SDF-1/CXCR4 interaction is primarily required for recruiting BMDCs, leading to neovasculogenesis in recurrent GBM. Therefore, inhibition of the SDF-1/CXCR4 interaction might be a promising strategy against the recurrence of GBM [34, 35]. Our data show that the expression of the SASP genes MCP1, GRO1, IL6, IL8, IL1α, and IL1β was significantly increased in irradiated GBM cells. Previous studies have demonstrated that these SASP factors are strongly associated with the tumor microenvironment and tumor progression. For example, MCP1, also known as CCL2, is important for recruiting monocytes, which promote breast cancer metastasis and correlate with poor prognosis [36, 37]. GRO1 promotes the migration of prostate cancer cells [38]. IL6 and IL8 secreted by senescent cells stimulate the invasion of premalignant cells [23]. Therefore, it is likely that targeting therapy-induced cellular senescence or SASP would be a promising approach to improve the therapeutic response and survival rate of cancer patients.

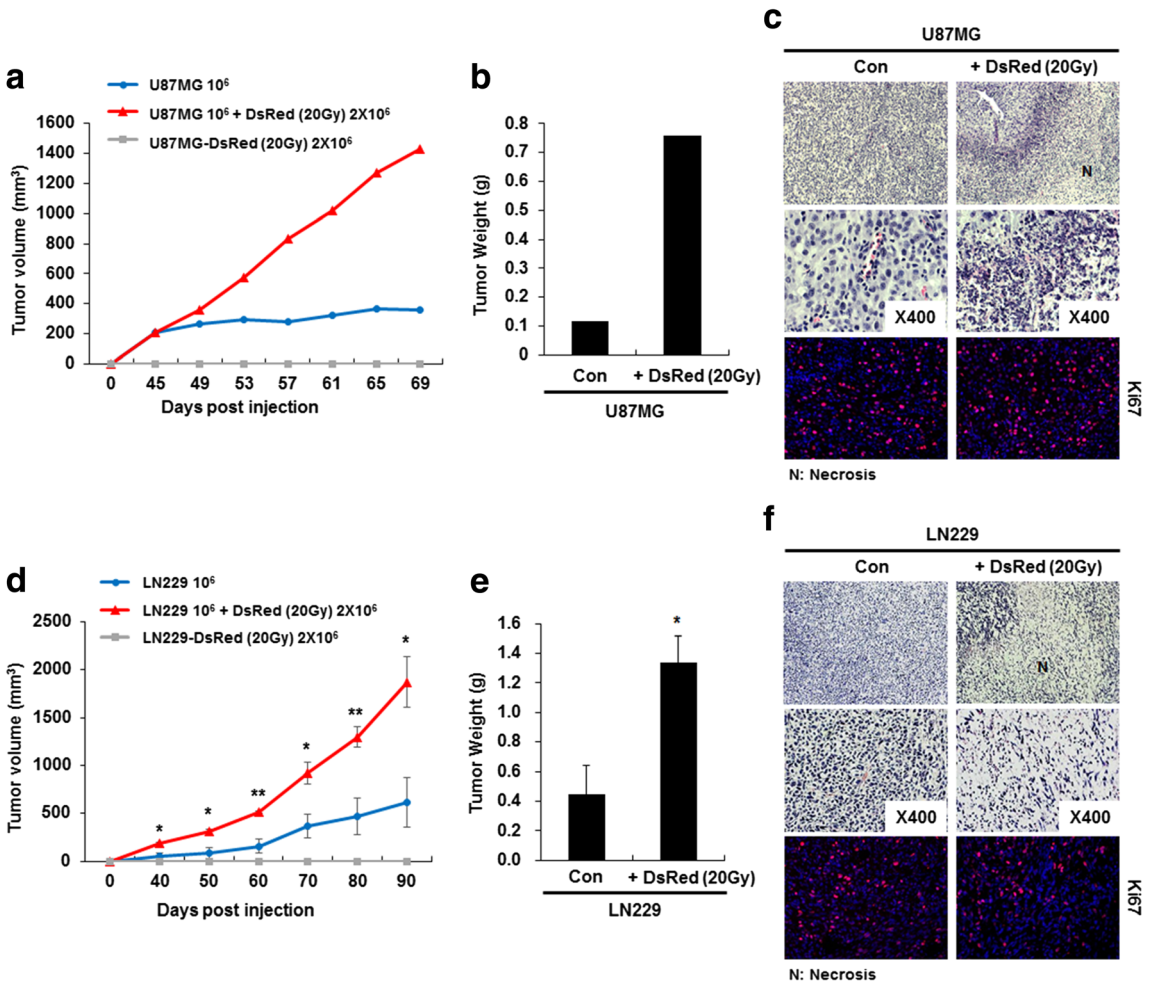


**Fig. 6** Irradiated GBM cells promote tumor xenograft growth of non-irradiated GBM cells. **a** and **d** No tumor growth was observed after injection of irradiated GBM cells in immune-deficient mice (**a**, U87MG and **d**, LN229). The larger tumor volume was formed by co-injection of non-irradiated GBM and irradiated GBM cells at a ratio of 1:2 compared to injection of non-irradiated GBM cells alone (**a**, U87MG cells and **d**, LN229 cells). *$p<0.05$, **$p<0.01$ ($n$ for U87MG cells=2, $n$ for LN229 cells=4). Data are expressed as means±SEM. **b** and **e** Tumor weight was increased by co-injection of non-irradiated GBM and irradiated GBM cells compared to injection of non-irradiated GBM cells alone. The mice were sacrificed on day 69 (**b**, U87MG cells) and day 90 (**e**, LN229 cells). *$p<0.05$ ($n$=4). Data are expressed as means±SEM. **c** and **f** H&E and Ki67 staining revealed that tumors derived from co-injection of non-irradiated GBM and irradiated GBM cells showed histological features of human GBM compared to tumors derived from injection of non-irradiated GBM cells alone. The mice were sacrificed on day 69 (**c**, U87MG cells) and day 90 (**f**, LN229 cells). *N* necrosis. The images shown are 400× magnified

Activated NFκB signaling has been detected in several types of solid tumors, including breast tumors, prostate tumors, melanoma, and GBM [39–41]. NFκB signaling is involved in tumor cell proliferation, invasion, angiogenesis, and inflammation. Activation of NFκB signaling is a major signaling mechanism that triggers SASP induction and likely generates a favorable microenvironment for the recurrence observed in GBM. Therefore, our study suggests that the combination of standard therapy with the targeting of NFκB signaling is an attractive therapeutic strategy to suppress tumor progression and recurrence through inhibition of SASP-driven changes in the tumor microenvironment.

**Acknowledgments** We would like to thank all the members of the Cell Growth Regulation Laboratory for their helpful discussion and technical assistance. This work was supported by the National Nuclear Technology Program through the National Research Foundation (NRF) of Korea funded by the Ministry of Science, ICT, and Future Planning (No. 2013M2A2A7042530 to H. Kim), and a research grant (to S.Y. Oh) funded by the Institute of Life Science and Natural Resources at Korea University.

**Compliance with ethical standards** The study experiments were approved by the Animal Care Committee of the College of Life Sciences and Biotechnology, Korea University, according to government and institutional guidelines and regulations of Korea.

**Conflicts of interest** None.

## References

1. Wen PY, Kesari S. Malignant gliomas in adults. N Engl J Med. 2008;359:492–507.
2. Stupp R, Mason WP, Van Den Bent MJ, Weller M, Fisher B, Taphoorn MJ, et al. Radiotherapy plus concomitant and adjuvant temozolomide for glioblastoma. N Engl J Med. 2005;352:987–96.
3. Grossman SA, Ye X, Piantadosi S, Desideri S, Nabors LB, Rosenfeld M, et al. Survival of patients with newly diagnosed glioblastoma treated with radiation and temozolomide in research studies in the United States. Clin Cancer Res. 2010;16:2443–9.
4. Liang BC, Thornton Jr AF, Sandler HM, Greenberg HS. Malignant astrocytomas: focal tumor recurrence after focal external beam radiation therapy. J Neurosurg. 1991;75:559–63.
5. Sneed PK, Gutin PH, Larson DA, Malec MK, Phillips TL, Prados MD, et al. Patterns of recurrence of glioblastoma multiforme after external irradiation followed by implant boost. Int J Radiat Oncol Biol Phys. 1994;29:719–27.
6. Chang JE, Khuntia D, Robins HI, Mehta MP. Radiotherapy and radiosensitizers in the treatment of glioblastoma multiforme. Clin Adv Hematol Oncol. 2007;894–902:7–15.
7. Tanaka S, Louis DN, Curry WT, Batchelor TT, Dietrich J. Diagnostic and therapeutic avenues for glioblastoma: no longer a dead end? Nat Rev Clin Oncol. 2013;10:14–26.
8. Persano L, Rampazzo E, Basso G, Viola G. Glioblastoma cancer stem cells: role of the microenvironment and therapeutic targeting. Biochem Pharmacol. 2013;85:612–22.
9. Mitchell JB, Choudhuri R, Fabre K, Sowers AL, Citrin D, Zabludoff SD, et al. In vitro and in vivo radiation sensitization of human tumor cells by a novel checkpoint kinase inhibitor, AZD7762. Clin Cancer Res. 2010;16:2076–84.
10. Bernhard EJ, Maity A, Muschel RJ, McKenna WG. Effects of ionizing radiation on cell cycle progression. Radiat Environ Biophys. 1995;34:79–83.
11. Maity A, McKenna WG, Muschel RJ. The molecular basis for cell cycle delays following ionizing radiation: a review. Radiother Oncol. 1994;31:1–13.
12. Campisi J, di Fagagna FA. Cellular senescence: when bad things happen to good cells. Nat Rev Mol Cell Biol. 2007;8:729–40.
13. Roninson IB. Tumor cell senescence in cancer treatment. Cancer Res. 2003;63:2705–15.
14. Bravata V, Minafra L, Russo G, Forte GI, Cammarata FP, Ripamonti M, et al. High-dose ionizing radiation regulates gene expression changes in the MCF7 breast cancer cell line. Anticancer Res. 2015;35:2577–91.
15. Ye C, Zhang X, Wan J, Chang L, Hu W, Bing Z, et al. Radiation-induced cellular senescence results from a slippage of long-term G2 arrested cells into G1 phase. Cell Cycle. 2013;12:1424–32.
16. Hornsby PJ. Senescence as an anticancer mechanism. J Clin Oncol. 2007;25:1852–7.
17. Wu C-H, van Riggelen J, Yetil A, Fan AC, Bachireddy P, Felsher DW. Cellular senescence is an important mechanism of tumor regression upon c-Myc inactivation. Proc Natl Acad Sci U S A. 2007;104:13028–33.
18. Cerella C, Grandjenette C, Dicato M, Diederich M. Roles of apoptosis and cellular senescence in cancer and aging. Curr Drug Targets. 2015.
19. Acosta JC, Banito A, Wuestefeld T, Georgilis A, Janich P, Morton JP, et al. A complex secretory program orchestrated by the inflammasome controls paracrine senescence. Nat Cell Biol. 2013;15:978–90.
20. Rodier F, Campisi J. Four faces of cellular senescence. J Cell Biol. 2011;192:547–56.
21. Han NK, Kim BC, Lee HC, Lee YJ, Park MJ, Chi SG, et al. Secretome analysis of ionizing radiation-induced senescent cancer cells reveals that secreted rkip plays a critical role in neighboring cell migration. Proteomics. 2012;12:2822–32.
22. Acosta JC, O'Loghlen A, Banito A, Guijarro MV, Augert A, Raguz S, et al. Chemokine signaling via the CXCR2 receptor reinforces senescence. Cell. 2008;133:1006–18.
23. Coppe JP, Patil CK, Rodier F, Sun Y, Munoz DP, Goldstein J, et al. Senescence-associated secretory phenotypes reveal cell-nonautonomous functions of oncogenic RAS and the p53 tumor suppressor. PLoS Biol. 2008;6:2853–68.
24. Liao EC, Hsu YT, Chuah QY, Lee YJ, Hu JY, Huang TC, et al. Radiation induces senescence and a bystander effect through metabolic alterations. Cell Death Dis. 2014;5, e1255.
25. Mosieniak G, Strzeszewska A. The role of cellular senescence in carcinogenesis and antitumor therapy. Postepy Biochem. 2014;60:194–206.
26. Petit V, Massonnet G, Maciorowski Z, Touhami J, Thuleau A, Nemati F, et al. Optimization of tumor xenograft dissociation for the profiling of cell surface markers and nutrient transporters. Lab Investig. 2013;93:611–21.
27. Vogelstein B, Lane D, Levine AJ. Surfing the p53 network. Nature. 2000;408:307–10.
28. Pyrko P, Soriano N, Kardosh A, Liu Y-T, Uddin J, Petasis NA, et al. Downregulation of survivin expression and concomitant induction of apoptosis by celecoxib and its non-cyclooxygenase-2-inhibitory analog, dimethyl-celecoxib (DMC), in tumor cells in vitro and in vivo. Mol Cancer. 2006;5:19.
29. Chien Y, Scuoppo C, Wang X, Fang X, Balgley B, Bolden JE, et al. Control of the senescence-associated secretory phenotype by NF-κB promotes senescence and enhances chemosensitivity. Genes Dev. 2011;25:2125–36.

30. Bartkova J, Hořejší Z, Koed K, Krämer A, Tort F, Zieger K, et al. DNA damage response as a candidate anti-cancer barrier in early human tumorigenesis. Nature. 2005;434:864–70.
31. Michaloglou C, Vredeveld LC, Soengas MS, Denoyelle C, Kuilman T, van der Horst CM, et al. BRAFE600-associated senescence-like cell cycle arrest of human naevi. Nature. 2005;436:720–4.
32. Krtolica A, Parrinello S, Lockett S, Desprez PY, Campisi J. Senescent fibroblasts promote epithelial cell growth and tumorigenesis: a link between cancer and aging. Proc Natl Acad Sci U S A. 2001;98:12072–7.
33. Stupp R, Hegi ME, Mason WP, van den Bent MJ, Taphoorn MJ, Janzer RC, et al. Effects of radiotherapy with concomitant and adjuvant temozolomide versus radiotherapy alone on survival in glioblastoma in a randomised phase III study: 5-year analysis of the EORTC-NCIC trial. Lancet Oncol. 2009;10:459–66.
34. Yang I, Aghi MK. New advances that enable identification of glioblastoma recurrence. Nat Rev Clin Oncol. 2009;6:648–57.
35. Liu SC, Alomran R, Chernikova SB, Lartey F, Stafford J, Jang T, et al. Blockade of SDF-1 after irradiation inhibits tumor recurrences of autochthonous brain tumors in rats. Neuro Oncol. 2014;16:21–8.
36. Qian B-Z, Li J, Zhang H, Kitamura T, Zhang J, Campion LR, et al. CCL2 recruits inflammatory monocytes to facilitate breast-tumour metastasis. Nature. 2011;475:222–5.
37. Lu X, Kang Y. Chemokine (C-C motif) ligand 2 engages CCR2+ stromal cells of monocytic origin to promote breast cancer metastasis to lung and bone. J Biol Chem. 2009;284:29087–96.
38. Kuo PL, Shen KH, Hung SH, Hsu YL. CXCL1/GROalpha increases cell migration and invasion of prostate cancer by decreasing fibulin-1 expression through NF-kappaB/HDAC1 epigenetic regulation. Carcinogenesis. 2012;33:2477–87.
39. Karin M, Cao Y, Greten FR, Li ZW. NF-kappaB in cancer: from innocent bystander to major culprit. Nat Rev Cancer. 2002;2:301–10.
40. Kim HJ, Hawke N, Baldwin AS. NF-kappaB and IKK as therapeutic targets in cancer. Cell Death Differ. 2006;13:738–47.
41. Atkinson GP, Nozell SE, Benveniste ET. NF-kappaB and STAT3 signaling in glioma: targets for future therapies. Expert Rev Neurother. 2010;10:575–86.